Singularities in the X-Ray Absorption and Emission of Metals. II. Self-Consistent Treatment of Divergences

P. NOZIÈRES*
University of California, San Diego, La Jolla, California 92037

AND

J. GAVORET AND B. ROULET
Groupe de Physique des Solides ENS,† Faculté des Sciences de Paris, 9, Quai Saint Bernard, Paris (5e), France

(Received 22 August 1968)

The many-body approach of the preceding paper is generalized to include self-energy and vertex renormalization is self-consistent fashion. The algebra of parquet diagrams is developed in terms of an unknown divergent parameter (related to the deep-hole Green's function $\mathcal{G}$), and of an unknown irreducible interaction R. The resulting interaction operator γ is used to calculate $\mathcal{G}$ and R; the corresponding coupled equations are solved self-consistently in the weak coupling limit. The spectral densities of the deep-hole Green's function and of the x-ray response function are calculated explicitly; in the weak coupling limit, the Mahan singularity found in the preceding paper is unaffected by renormalization. The self-consistent formalism presented here describes the reaction of divergent fluctuations on themselves, and should, therefore, be useful in other more complicated problems, such as the Kondo effect.

I. INTRODUCTION

IN the preceding paper,[1] the problem of x-ray absorption and emission in metals was studied by the methods of perturbation theory. Assuming that such effects as lifetime and recoil of the localized deep hole may be neglected, we showed that the spectrum should display a marked singularity near the Fermi level threshold, in agreement with the prediction of Mahan.[2] In this paper, we wish to pursue further the mathematical analysis of the problem; for all physical discussions, the reader is referred to I.

Let us briefly formulate the problem again. We denote by $a_{\mathbf{k}}^\dagger$ and $\epsilon_{\mathbf{k}}$ the creation operator and energy of conduction electrons. The deep level involved in the x-ray transition is assumed to be localized, with a creation operator $b^\dagger$ and unrenormalized energy E_0. We only consider the *intraband* part of the Coulomb interaction, involving transitions in which the deep level is unchanged, while the conduction remains in the same band. We thus work with the model Hamiltonian.

$$H=\sum_{\mathbf{k}} \epsilon_{\mathbf{k}} a_{\mathbf{k}}^\dagger a_{\mathbf{k}} + E_0 b^\dagger b + \sum_{\mathbf{k}\mathbf{k}'} V_{\mathbf{k}\mathbf{k}'} a_{\mathbf{k}}^\dagger a_{\mathbf{k}'} b b^\dagger . \quad (1)$$

At the moment, the electron spin is ignored; we shall restore it at the end by adding the relevant factors 2. In order to solve the equations, we use a separable potential of the form

$$\begin{aligned} V_{\mathbf{k}\mathbf{k}'} &= -V u_{\mathbf{k}} u_{\mathbf{k}'} , \\ u_{\mathbf{k}} &= 1, \quad \text{if} \quad |\epsilon_{\mathbf{k}}-\mu| < \xi_0 \\ &= 0, \quad \text{otherwise.} \end{aligned} \quad (2)$$

μ is the chemical potential, ξ_0 a cutoff of order μ. With this definition, V is positive, corresponding to an attraction between conduction electrons and the deep hole. The basic dimensionless parameter of the theory is

$$g=\nu_0 V ,$$

where ν_0 is the density of states at the Fermi surface (for one spin). We assume that $g \ll 1$.

The x-ray transition rate may be obtained from the imaginary part of a response function $\chi(\omega)$, which is the Fourier transform of[3]

$$\begin{aligned} \chi(t-t') &= \langle 0 | T\{A(t)A(t')\} | 0 \rangle , \\ A &= \sum_{\mathbf{k}} u_{\mathbf{k}} a_{\mathbf{k}}^\dagger b + \text{c.c.} \end{aligned} \quad (3)$$

In perturbation theory, $\chi(\omega)$ is given by all graphs of Fig. 1, summed over $\mathbf{k}$, $\mathbf{k}'$, ϵ, ϵ'. Dashed and full lines represent, respectively, the renormalized deep-level and conduction-electron Green's functions, defined as

$$\begin{aligned} \mathcal{G}(t-t') &= i\langle 0 | T\{b(t)b^\dagger(t')\} | 0 \rangle , \\ G_{\mathbf{k}\mathbf{k}'}(t-t') &= i\langle 0 | T\{a_{\mathbf{k}}(t) a_{\mathbf{k}'}^\dagger(t')\} | 0 \rangle \end{aligned} \quad (4)$$

(as usual, T is the chronological operator, and $|0\rangle$ represents the exact "ground state," with the deep level either full or empty for the absorption or emission

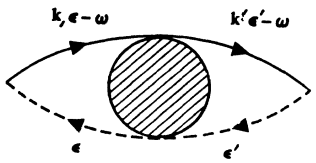

FIG. 1. Graphs contributing to the response function $\chi(\omega)$.

* NSF Senior Foreign Scientist Fellow. Permanent address: Groupe de Physique des Solides ENS, Faculté des Sciences, 9 Quai Saint Bernard, Paris, France.

† Laboratoire Associé au Centre National de la Recherche Scientifique.

[1] B. Roulet, J. Gavoret, and P. Nozières, preceding paper, Phys. Rev. 178, 1078 (1969), hereafter referred to as I.

[2] G. D. Mahan, Phys. Rev. 163, 612 (1967).

[3] As in the preceding paper, we take a constant x-ray matrix element cutoff for $(\epsilon_{\mathbf{k}}-\mu) > \xi_0$. Such a cutoff does not affect the x-ray spectrum near threshold, see I, Ref. 10.

cases). Our purpose is to calculate $\chi(\omega)$ (which is directly measurable) and $\mathcal{G}(\epsilon)$ (which, although not measurable, has some theoretical interest).

The interaction term of (1) modifies the energy of the deep level. The spectrum of $\mathcal{G}$ is *shifted* (its branch point lying now at an energy $E\neq E_0$), and *broadened asymmetrically* (through excitation of conduction electrons). The broadening extends to the low- or high-energy side of E, respectively, for the absorption or emission case. The deep Green's function $\mathcal{G}$ always runs in the same direction of time (because there is only *one* deep level). Thus, there is only one open dashed line throughout any diagram, and no dashed closed loop. This allows us to choose independently the energy origins for conduction and deep electrons. We measure the conduction-electron energy from μ and the deep-electron energy from E; and thus, the x-ray frequency ω from its threshold value $\omega_0=\mu-E$. Throughout the paper we make the replacement

$$\begin{aligned} \epsilon-\mu,\ \epsilon_k-\mu &\longrightarrow \epsilon,\ \epsilon_k, && \text{conduction electrons}\\ \epsilon-E &\longrightarrow \epsilon, && \text{deep electron}\\ \omega-\omega_0 &\longrightarrow \omega, && \text{x-ray frequency.}\end{aligned}$$

By doing so, we ignore the shift of the threshold, which is incorporated in the choice of origin. The branch point of $\mathcal{G}$ now lies at $\epsilon=0$, which means that the self-energy Σ should actually be replaced by

$$\bar{\Sigma}(\epsilon)=\Sigma(\epsilon)-\Sigma(0). \tag{5}$$

The calculation of the shift $(E-E_0)$ is difficult in the present formalism, and will be relegated to a further paper using a different approach.[4]

Because of our choice of a separable interaction (2) the momentum variables are completely decoupled. The perturbation expansion involves only the following combination of conduction-electron Green's functions:

$$G(\epsilon)=\sum_{kk'} u_k u_{k'} G_{kk'}(\epsilon). \tag{6}$$

Our problem thus involves only one dimension: the energy.

The Mahan singularity arises from a resonance in the general interaction operator γ given by all graphs of Fig. 2(a). It is convenient to express γ as a function of the two deep-level energies ϵ_1 and ϵ_2 and of either of the total energies in the two singular channels

$$\begin{aligned}\xi&=\epsilon_1+\epsilon_1'=\epsilon_2+\epsilon_2',\\ \eta&=\epsilon_1-\epsilon_2'=\epsilon_2-\epsilon_1'.\end{aligned}$$

As in I, we shall use different notations to distinguish between the two sets of variables

$$\gamma=\gamma(\epsilon_1,\epsilon_2,\xi)=\bar{\gamma}(\epsilon_1,\epsilon_2,\eta). \tag{7}$$

The resonant singularity already appears in the second-order graphs shown on Fig. 2(b) and 2(c), which are

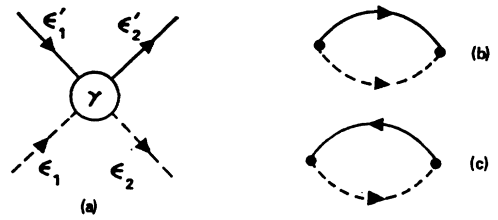

FIG. 2. (a) The most general graph contributing to the interaction operator γ (b) and (c). The two-second order terms of γ.

logarithmically divergent when $\xi,\eta\to 0$. The existence of these two singular "bubbles" makes it necessary to study multiple scattering in the corresponding two channels. One is thus led to write two coupled Bethe-Salpeter equations, the so-called "parquet" equations derived in Sec. IV of I. In these equations, γ is expressed in terms of the Green's functions G, $\mathcal{G}$, and of a *totally irreducible* interaction R (i.e., irreducible in the two singular channels).

The perturbation expansion may be expressed in terms of two parameters: the coupling constant g and the product gL, where L is any of the divergent logarithms. Thus, γ has the form

$$\gamma=V[\alpha_0(gL)+g\alpha_1(gL)+g^2\alpha_2(gL)\cdots].$$

The preceding paper was devoted to the leading approximation, in which only the term α_0 is retained. Such an approximation, valid if $g\ll 1$, $gL\lesssim 1$, clearly breaks down when $gL\gg 1$ (for instance, a quantity like g^2L, belonging to α_1, may become larger than 1). In the limit $L\to\infty$ (i.e., $\epsilon\to 0$), we must reconsider our whole expansion; we need a new criterion to select the relevant perturbation graphs. In this paper, we develop a more refined formalism which is valid down to $\epsilon=0$. The major difference from I is a *self-consistent renormalization* of all singularities, which allows for the reaction of divergent fluctuations on themselves. Such an approach goes beyond the usual parquet theory, as applied, for instance, to high-energy meson scattering,[5,6] to the Kondo effect[7] and to one-dimensional superconductivity.[8] It is hoped that the method as such may prove useful in these more complicated problems, especially in the Kondo effect (as we shall see, the x-ray problem is particularly simple, because of strong cancellation between divergent factors). This is, in fact, the main motivation of the paper, since the problem under study may be solved exactly by a much simpler method.[4]

In Sec. II, we review the main approximations of I, and we show how they can be formally avoided by

[4] P. Nozières and C. T. de Dominicis, following paper, Phys. Rev. **178**, 1097 (1969).

[5] V. V. Sudakov, Dokl. Akad. Nauk SSSR **111**, 338 (1956) [English transl.: Soviet Phys.—Doklady **1**, 662 (1956)].

[6] I. T. Diatlov, V. V. Sudakov, K. A. Ter-Martirosian, Zh. Eksperim. i Teor. Fiz. **32**, 767 (1957) [English transl.: Soviet Phys.—JETP **5**, 631 (1957)].

[7] A. A. Abrikosov, Physics **2**, 5 (1965).

[8] Yu A. Bychkov, L. P. Gor'kov, and I. E. Dzyaloshinski, Zh. Eksperim. i Teor. Fiz. **50**, 738 (1966) [English transl.: Soviet Phys.—JETP **23**, 489 (1966)].

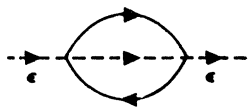

FIG. 3. The lowest-order graphs for the self-energy Σ.

introducing an unknown divergent factor and an unknown interaction R. In Sec. III, we solve the parquet equations and express γ in terms of these unknown quantities. In Sec. IV, the self-energy Σ is evaluated (near the branch point) in terms of γ. The irreducible interaction R is shown to be closely related to Σ, through the same conservation laws that lead to Ward identities. It is thus essential to maintain *consistent approximations* in the calculation of Σ and R. The preceding analysis leads to a set of coupled equations which are solved in Sec. V. The physical implications of the solution are described in Sec. VI, together with possible generalizations of the theory. The validity of our approximations is discussed in the appendices.

II. APPROXIMATIONS OF ELEMENTARY PARQUET THEORY

We start from the exact parquet equations (I.20) and (I.21) established in the preceding paper.[9]

$$\gamma_1(\epsilon_1,\epsilon_2,\xi)=\frac{i}{2\pi}\int d\epsilon_i I_1(\epsilon_1,\epsilon_i,\xi)\mathcal{G}(\epsilon_i)G(\xi-\epsilon_i)\gamma(\epsilon_i,\epsilon_2,\xi)\,, \tag{8}$$

$$\bar{\gamma}_2(\epsilon_1,\epsilon_2,\eta)=\frac{i}{2\pi}\int d\epsilon_i \bar{I}_2(\epsilon_1,\epsilon_i,\eta)\mathcal{G}(\epsilon_i)G(\epsilon_i-\eta)\bar{\gamma}(\epsilon_i,\epsilon_2,\eta)\,,$$

$$I_1=R+\gamma_2\,,\quad I_2=R+\gamma_1\,,\quad \gamma=R+\gamma_1+\gamma_2\,. \tag{9}$$

I_1 and I_2 are *irreducible* interactions in channels 1 and 2, while γ_1 and γ_2 are the *reducible* interactions in the two channels. The conduction-electron Green's function is given by (I.12):

$$\begin{aligned} &G(\epsilon)=\nu_0 f_0/(1-gf_0)\,,\\ &f_0(\epsilon)=\ln|(\xi_0-\epsilon)/(\xi_0+\epsilon)|+i\pi\theta(\epsilon)\,,\\ &\theta(\epsilon)=\operatorname{sgn}\epsilon \text{ if } |\epsilon|<\xi_0\,,\ =0 \text{ if } |\epsilon|>\xi_0\,. \end{aligned} \tag{10}$$

The deep-level Green's function is

$$\mathcal{G}(\epsilon)=-1/[\epsilon+\tilde{\Sigma}(\epsilon)]\,, \tag{11}$$

where $\tilde{\Sigma}(\epsilon)$ is the reduced self-energy [see (5)]. Until now, no approximation has been made.

In the course of our first-order parquet calculation, we made *four* independent approximations:

(a) neglect of the deep-level self-energy $\tilde{\Sigma}$,
(b) neglect of all terms of R but the first order one: $R\to V$,
(c) approximation on the conduction-electron Green's function G, amounting to the replacement

$$\begin{aligned} G(\xi-\epsilon_i)&\to -i\pi\nu_0\operatorname{sgn}\epsilon_i\,, \text{ if } |\xi|<|\epsilon_i|<\xi_0\\ &\to 0\,, \qquad\qquad \text{otherwise.} \end{aligned} \tag{12}$$

(By doing so we lose the contribution of the δ function arising from $\operatorname{Im}\mathcal{G}$.),
(d) replacement of the irreducible interactions I_1 and I_2 by the simplified form (I.31)

$$\begin{aligned} I_1(\epsilon_1,\epsilon_i,\xi)&=V+\bar{\gamma}_2[\max(\epsilon_1,\epsilon_i)]\,,\\ \bar{I}_2(\epsilon_1,\epsilon_i,\eta)&=V+\gamma_1[\max(\epsilon_1,\epsilon_i)] \end{aligned} \tag{13}$$

[where $\gamma(\epsilon)$ is a shorthand notation for $\gamma(\epsilon,\epsilon,\epsilon)$].

These approximations being granted, the parquet equations (8) and (9) were solved *exactly*. The whole problem lies in an appraisal of approximations (a) to (d). We saw that they provided the leading order of the parquet expansion in powers of g; in that respect, they represent a *well-defined* degree of accuracy. We shall now question them successively.

The lowest-order term of $\tilde{\Sigma}$ is obtained from the graph of Fig. 3. Its calculation is straightforward. On making use of (5), we find

$$\tilde{\Sigma}^{(2)}(\epsilon)\sim g^2\epsilon\ln(\xi_0/\epsilon)\,.$$

Such a correction must be compared to ϵ; it will become important when $g^2L\gtrsim 1$. In principle, there could exist higher-order terms of the form

$$\tilde{\Sigma}\sim\epsilon g^{n+l}L^n\,,$$

which would become relevant for even smaller values of L. We shall see in Sec. IV that such terms do not occur. We thus conclude that the renormalization of $\mathcal{G}$ is important only for very small energies $\epsilon\gtrsim\xi_0\times\exp[-1/g^2]$, way below the characteristic energies in the x-ray singularity.

The behavior of $\mathcal{G}$ determines the nature of singularities in the perturbation expansion. The basic divergence arising from singular bubbles involves the integral

$$l(\epsilon)=-\int_{\epsilon}^{\xi_0}\mathcal{G}(\epsilon')d\epsilon'\,. \tag{14}$$

When $\mathcal{G}$ is not renormalized, l reduces to the usual

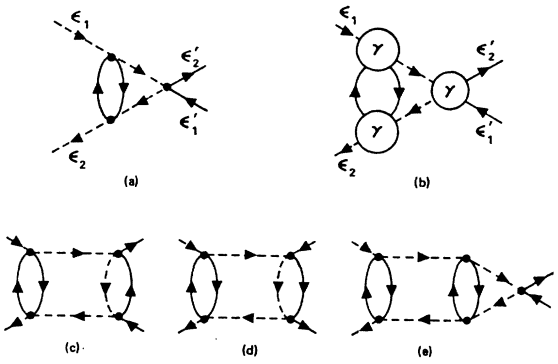

FIG. 4. (a) The third-order correction to the irreducible interaction R. (b) A general graph constructed by renormalizing the vertices of Fig. 4(a). Examples of such graphs are obtained by replacing the right-hand-side vertex of Fig. 4(a) by either type of singular bubble [4(c) and 4(d)] or by the diagram 4(a) itself 4(e).

[9] Throughout the paper, we refer to the equations of the preceding paper by a prefix I.

logarithmic factor $\ln(\xi_0/\epsilon)$. If, however, Σ builds up, $\mathcal{G}$ is smaller, and the integral (14) is less divergent. Renormalization of $\mathcal{G}$ will, therefore, make the factors $t(\epsilon)$ *less singular*. We are then faced with an intricate problem:

(i) the singular factors t depend on Σ,
(ii) but Σ, in turn, depends on t.

Ultimately, these coupled equations must be solved self-consistently.

We remark that a change of t does not affect the algebra of parquet equations described in the preceding paper—as long as t remains a *large* and *slowly varying* function of ϵ. (The fact that singular factors were logarithms was in no way essential.) We may retain the calculations of I, the only difference being that t will now be some unknown function of ϵ, instead of a logarithm. (The so-called "logarithmic" approximation is actually an approximation for slowly varying functions.) The interaction operator γ will appear as a function of the unknown quantity t.

We now turn to the totally irreducible interaction R. The lowest-order correction corresponds to the graph of Fig. 4(a), whose contribution is found to be

$$R^{(3)}(\epsilon_1,\epsilon_2,\epsilon_1',\epsilon_2')\sim Vg^2\frac{\epsilon_1\ln(\xi_0/\epsilon_1)-\epsilon_2\ln(\xi_0/\epsilon_2)}{\epsilon_1-\epsilon_2}. \quad (15)$$

To the extent that $\epsilon_1,\epsilon_2\ll\xi_0$, and within our logarithmic accuracy, we may replace (15) by

$$R^{(3)}\sim Vg^2\ln\left[\frac{\xi_0}{\max(\epsilon_1,\epsilon_2)}\right]. \quad (16)$$

As compared to the first-order term V the correction (16) becomes important when $g^2L\gtrsim 1$: The sort of vertex renormalization described by Fig. 4(a) must be treated on the same footing as self-energy renormalization.

Among the higher-order terms of R, we consider first the graphs obtained by *renormalizing* the vertices of Fig. 4(a), i.e., replacing them by a full interaction operator γ [see Fig. 4(b)]. The first correction is obtained by replacing any vertex by a singular bubble of either type 2(b) or 2(c) [as done for instance on Fig. 4(c) and 4(d)]. The additional bubble gives rise to an extra logarithm factor: The contribution of *each* of these terms is $\sim Vg^3L^2$. We should, however, realize that the energies entering the two channels of the replaced vertex are comparable (they are integration variables). Hence, the two types of singular bubbles cancel out, and the *sum* of the two graphs 4(b) and 4(c) contains only one logarithm, being $\sim\frac{1}{2}g^3L$. However small the energy, such a contribution is negligible as compared to the third-order term (16). More generally, we get no sizable correction when replacing all three vertices of Fig. 4(a) by the elementary parquet graphs of the preceding paper, since we know that for equal energies in the two channels, the sum of these graphs reduces to

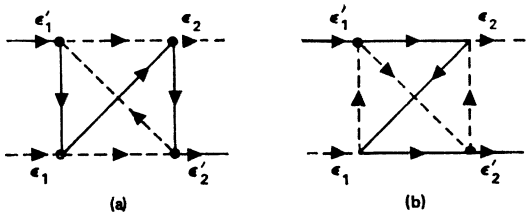

FIG. 5. Fourth-order "nonparquet" graphs.

the first-order term V. On the other hand, let us replace a vertex of Fig. 4(a) by the diagram 4(a) itself, as done in Fig. 4(e); the corresponding contribution turns out to be $\sim Vg^4L^2$ (see Appendix A): Here, there is one extra logarithm which does not cancel out. Such a contribution may be comparable to, or even larger than (16). We must, therefore, retain the general class of diagrams of Fig. 4(b), keeping in mind that it will be the nonparquet part of the three factors γ that will lead to sizable corrections. One may prove by induction that the conduction-electron energies ϵ_1' and ϵ_2', which do not enter the third-order term (16), do not enter either the sum of all graphs 4(b). Within logarithmic accuracy, the corresponding contribution to R will thus be a function only of $\max(\epsilon_1,\epsilon_2)$. (This contention will be substantiated by the final result.) We note that the above discussion strongly suggests that the expansion parameter for nonparquet graphs is g^2L rather than gL.

Figure 4(b) in no way exhausts the possible graphs for R. In fourth order, for instance, we find the two graphs[10] of Fig. 5 whose contribution $\sim Vg^3L$ is negligible as compared to (16). A complete analysis is carried out in Appendix A, where we conclude that all these higher "nonparquet" graphs are negligible as long as $g\ll 1$ (the simplification stems directly from the large cancellation of singularities between the two channels). In calculating R, we may restrict ourselves to the general graphs of Fig. 4(b)—in addition, of course, to the first-order vertex. R appears as a function of γ, which again must be obtained self-consistently.

The last approximations (c) and (d) may be viewed as calculational approximations to the kernels I and $G\mathcal{G}$ entering the exact Eqs. (8). The corresponding error in the interaction γ is evaluated in Appendix B. We show that the error on γ is, at most, of order g^2R, and is, therefore, negligible as compared to the main term (16).

Our theory will then proceed as follows:

(i) Start from the exact equations (8) and use the same logarithmic approximation as in I [stated in (12) and (13)]. Express the solution of (8) in terms of the *unknown* divergent parameter t and irreducible interaction R [assuming that R depends only on $\max(\epsilon_1\epsilon_2)$, that is on $\min(t_1,t_2)$].

[10] Actually, the two graphs of Figs. 5(a) and 5(b) cancel each other, because of the symmetry rule (I.22). Their net contribution is of order Vg^3 and involves no logarithm. The first logarithmic factor occurs through fifth order, and yields a result $\sim Vg^4L$.

(ii) From γ, calculate Σ and the main term of R [given by Fig. 4(b)].

(iii) Solve the resulting coupled equations, which yield first the explicit form $R(t)$, and then the behavior of $t(\epsilon)$.

Ultimately, the results of the theory must be used to check the validity of all our approximations.

III. CALCULATION OF INTERACTION OPERATOR AND RESPONSE FUNCTION

We replace all energy variables ϵ_1, ϵ_2, ϵ_i, ξ, η by the corresponding quantities t_1, t_2, t_i, α, β defined in (14). t is no longer a logarithm, but is still *slowly* varying. We notice that the energy variables are not independent ($\epsilon_1+\epsilon_2=\xi+\eta$); hence, we still have a relation similar to (I.33):

$$\min(t_1,t_2)=\min(\alpha,\beta). \tag{17}$$

With these new variables, the basic equations (8) become [see (I.34)]:

$$\begin{aligned}\gamma_1(t_1,t_2,\alpha)&=-\nu_0\int_0^\alpha dt_i I_1(\min(t_1,t_i))\\&\quad\times\{I_1(\min(t_2,t_i))+\gamma_1(t_i,t_2,\alpha)\},\\ \bar\gamma_2(t_1,t_2,\beta)&=+\nu_0\int_0^\beta dt_i \bar I_2(\min(t_1,t_i))\\&\quad\times\{\bar I_2(\min(t_2,t_i))+\bar\gamma_2(t_i,t_2,\beta)\},\\ I_1(t)&=R(t)+\bar\gamma_2(t),\quad \bar I_2(t)=R(t)+\gamma_1(t).\end{aligned} \tag{18}$$

γ_1 or $\bar\gamma_2$ are iterations of kernels I_1 or $\bar I_2$, and are thus *symmetric* in the interchange of t_1 and t_2. We see on (18) that γ_1 does not depend on t_1 when $t_1>\alpha$ [in that case $\min(t_i t_i)=t_i$]: Hence, we can write, in shorthand notation,

$$\begin{aligned}\gamma_1(t_1,t_2,\alpha)&=\gamma_1(t_1,\alpha,\alpha)=\gamma_1(t_1,\alpha), \quad \text{if} \quad t_1<\alpha<t_2\\&=\gamma_1(\alpha,\alpha,\alpha)=\gamma_1(\alpha), \quad \text{if} \quad \alpha<t_1,t_2.\end{aligned} \tag{19}$$

A similar relation holds for $\bar\gamma_2$ (but *not* for R, which does not depend on α and β). Once γ_1 and γ_2 are known, the full interaction operator γ is obtained from

$$\gamma=\gamma_1+\gamma_2+R(\min(t_1,t_2)). \tag{20}$$

In order to solve Eqs. (18), we use the trick of Sudakov[5] and Abrikosov[7] described in the preceding paper. By selecting in any graph the intermediate bubble with the maxt_i, one may replace (18) by the strictly equivalent equations

$$\begin{aligned}\gamma_1(t_1,t_2,\alpha)&=-\nu_0\int_0^\alpha dt[I_1(\min(t_1,t))+\gamma_1(t_1,t,t)]\\&\quad\times[I_1(\min(t_2,t))+\gamma_1(t,t_2,t)],\\ \bar\gamma_2(t_1,t_2,\beta)&=+\nu_0\int_0^\beta dt[\bar I_2(\min(t_1,t))+\bar\gamma_2(t_1,t,t)]\\&\quad\times[\bar I_2(\min(t_2,t))+\bar\gamma_2(t,t_2,t)].\end{aligned} \tag{21}$$

The reader is referred to the Appendix of I for a proof of these equations. (21) will be solved by considering increasingly complicated cases:

(*i*) $t_1,t_2\gtrsim\alpha,\beta$. The general relation (17) then implies

$$\alpha=\beta=\min(t_1,t_2). \tag{22}$$

The various operators depend only on *one* variable, and the Eqs. (21) take the simple form

$$\bar\gamma_2(\alpha)=-\gamma_1(\alpha)=\nu_0\int_0^\alpha\gamma^2(t)dt. \tag{23}$$

Here again, there is complete cancellation between γ_1 and $\bar\gamma_2$ (the singularities in the two channels being opposite). The net operator γ contains only the irreducible part:

$$\gamma(\alpha)=R(\alpha). \tag{24}$$

(*ii*) $t_1<\alpha\lesssim t_2$. (17) then implies $\beta=t_1$, so that

$$\bar\gamma_2=\nu_0\int_0^{t_1}R^2(t)dt. \tag{25}$$

In (21), we separate the integration over t in two parts $(0,t_1)$ and (t_1,α). Making use of the previous result (24), we obtain

$$\gamma_1(t_1,\alpha)=-\nu_0\int_0^{t_1}R^2(t)dt-\nu_0\int_{t_1}^\alpha R(t)\gamma(t_1,t)dt. \tag{26}$$

A combination of (20), (25), and (26) leads to the following integral equation for γ:

$$\gamma(t_1,\alpha)=R(t_1)-\nu_0\int_{t_1}^\alpha R(t)\gamma(t_1,t)dt. \tag{27}$$

The solution of (27) is straightforward[11]; we find

$$\gamma(t_1,\alpha)=R(t_1)\exp\left[-\nu_0\int_{t_1}^\alpha R(t)dt\right]. \tag{28}$$

It is convenient to introduce the extra function

$$Q(t)=\nu_0\int_0^t R(t')dt'. \tag{29}$$

Remembering that here $t_1=\beta$, we can write (28) in the form

$$\gamma=R(\beta)e^{Q(\beta)-Q(\alpha)}. \tag{30}$$

A similar calculation in the case $\alpha=t_1<\beta\leq t_2$ would yield

$$\begin{aligned}\bar\gamma(t_1,\beta)&=R(t_1)\exp\left[+\nu_0\int_{t_1}^\beta R(t)dt\right]\\&=R(\alpha)e^{Q(\beta)-Q(\alpha)}.\end{aligned} \tag{31}$$

[11] We derive (27) with respect to α and integrate the resulting differential equation with the boundary condition $\gamma(t_1,t_1)=R(t_1)$.

The results (30) and (31) may be lumped into a single formula

$$\gamma = R(\min(\alpha,\beta))e^{Q(\beta)-Q(\alpha)} \quad \text{if} \quad t_1 < \max(\alpha,\beta) \leq t_2. \quad (32)$$

(*iii*) $t_1 < t_2 < \alpha$. Again, (17) implies $\beta = t_1$, and $\bar{\gamma}_2$ remains given by (25). In calculating γ_1, we separate the integration range of (21) into three parts $(0,t_1)$, (t_1,t_2), and (t_2,α). Since the γ which enter (21) always have two energies equal, they may be obtained from (28). We are left with straightforward integrations which yield

$$\gamma(t_1,t_2,\alpha) = R(t_1)e^{Q(t_1)-Q(t_2)} - \nu_0 R(t_1)R(t_2) \times \int_{t_2}^{\alpha} e^{Q(t_1)+Q(t_2)-2Q(t)}dt. \quad (33)$$

A similar calculation for $\alpha = t_1 < t_2 < \beta$ would lead to

$$\bar{\gamma}(t_1,t_2,\beta) = R(\min(t_1,t_2))e^{+|Q(t_2)-Q(t_1)|} + \nu_0 R(t_1)R(t_2) \times \int_{\max(t_1,t_2)}^{\beta} e^{2Q(t)-Q(t_1)-Q(t_2)}dt. \quad (34)$$

[In writing (34), we have allowed for possible permutation of t_1 and t_2.] The set of Eqs. (24), (32), (33), and (34) provide a complete solution. It is easily verified that they merge smoothly into each other—of course, they agree with the first-order result (I.35) if R is let equal to V.

From γ we may calculate the response function $\chi(\omega)$ given by (I.37). (As seen on Fig. 1, γ is simply sandwiched between two singular bubbles.) Including the zeroth-order term, χ is given by

$$\chi(\omega) = \nu_0\beta + \nu_0^2 \int_0^{\beta} dt_1 dt_2 \bar{\gamma}(t_1,t_2,\beta) \quad (35)$$

[compare with (I.38)]. Here β is the singular variable associated to the total energy ω. We replace $\bar{\gamma}$ by its expression (34), and use the symmetry of $\bar{\gamma}$ to write

$$\int_0^{\beta} dt_1 dt_2 = 2\int_0^{\beta} dt_2 \int_0^{t_2} dt_1.$$

We then integrate first over t_1, which yields (with obvious abbreviations)

$$\chi(\omega) = -\nu_0\beta + 2\nu_0 \int_0^{\beta} dt_2 e^{Q_2} + 2\nu_0 \int_0^{\beta} dt_2 R_2 \times \int_{t_2}^{\beta} dt\{e^{2Q-Q_2} - e^{2Q-2Q_2}\}.$$

Integrating the last term by parts over t_2, we finally obtain

$$\chi(\omega) = \nu_0 \int_0^{\beta} e^{2Q(t)}dt. \quad (36)$$

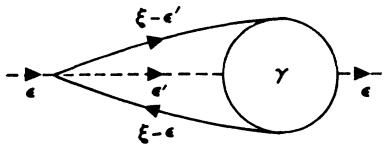

FIG. 6. Expression of the self-energy $\Sigma(\epsilon)$ in terms of the interaction operator γ.

(36) reduces to our former result (I.41) if R is replaced by V.

The two essential results of the section are (24) and (36). Let us emphasize again the cancellation of singular bubbles for equal energies, which persists even in the more sophisticated treatment. Such a cancellation simplifies the theory considerably.

IV. CALCULATION OF SELF-ENERGY AND IRREDUCIBLE INTERACTION

Let us isolate the entrance vertex of a self-energy graph, as shown in Fig. 6; in this way we can express Σ in terms of the interaction operator γ:

$$\Sigma(\epsilon) = -V\left(\frac{i}{2\pi}\right)^2 \int d\epsilon' d\xi G(\xi-\epsilon)G(\xi-\epsilon') \times \mathcal{G}(\epsilon')\gamma(\epsilon,\epsilon',\xi). \quad (37)$$

(Note the minus sign arising from the closed electron loop.) According to (37), it seems that Σ could be obtained from the results of Sec. III. Unfortunately, (37) is of no use, as it would require a knowledge of γ which goes beyond our logarithmic accuracy. In order to evaluate the singularity of $\mathcal{G}$, we need the reduced quantity $\tilde{\Sigma}$, given by (5)—or equivalently the derivative $\partial\Sigma/\partial\epsilon$ which determines the variation of Σ near its branch point. If we want to use (37), we must know the derivative $\partial\gamma/\partial\epsilon$, for which our logarithmic approximation is not reliable. [For instance, a term such as $\epsilon(\ln\epsilon)^n$, which would give a negligible contribution to γ, may be important in $\partial\gamma/\partial\epsilon$.] We must, therefore, abandon (37), and try to calculate $\partial\Sigma/\partial\epsilon$ *directly*.

For that purpose, we consider a *skeleton* graph of Σ (with all propagators renormalized), and we increase the external energy ϵ by a small amount $\delta\epsilon$. We may account for this change by increasing the energy of all internal *dashed* lines by the same amount $\delta\epsilon$. More generally, we may select an arbitrary path joining the entrance vertex to the exit vertex, involving some succession of dashed lines $\mathcal{G}_m$ and full lines G_n; when ϵ is increased by $\delta\epsilon$, each branch sees its energy ϵ_m modified by an amount $\eta_m\delta\epsilon$ ($\eta_m = \pm 1$, depending on the orientation of the particular branch along the path). The corresponding contribution to $\partial\Sigma/\partial\epsilon$ may be written as a sum over the whole path

$$\frac{\partial\Sigma}{\partial\epsilon} = \sum_m \frac{\delta\Sigma}{\delta\mathcal{G}_m}\eta_m\frac{\partial\mathcal{G}_m}{\partial\epsilon_m} + \sum_n \frac{\delta\Sigma}{\delta G_n}\eta_n\frac{\partial G_n}{\partial\epsilon_n}. \quad (38)$$

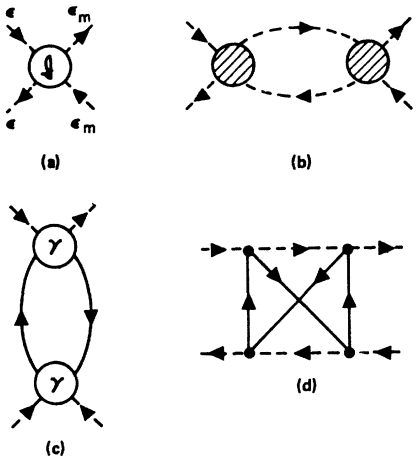

FIG. 7. (a) A general graph contributing to the irreducible interaction $\mathcal{I}$. (b) A *reducible* graph which does not belong to $\mathcal{I}$. (c) The graphs for $\mathcal{I}$ retained in our weak coupling approximation. (d) A higher-order graph of $\mathcal{I}$ whose contribution is negligible.

(Of course, there are many ways to draw such a path from entrance to exit: We must choose one and stick to it in order to avoid duplication.) We note that $\delta\Sigma/\delta G_n$ corresponds to a graph in which one internal *full* line of Σ has been open, i.e., to a graph of γ. Similarly, $\delta\Sigma/\delta\mathcal{G}_m$ is obtained by opening an internal *dashed* line, and thus corresponds to the four-dashed-line interaction graph of Fig. 7(a). Because we started from a skeleton self-energy graph, the diagrams of $\delta\Sigma/\delta G_n$ and $\delta\Sigma/\delta\mathcal{G}_m$ are always *irreducible* in the channel defined by the two external lines of Σ (they cannot be split by cutting two intermediate dotted lines). Thus, $\delta\Sigma/\delta\mathcal{G}_m$ explicitly excludes the reducible graphs shown in Fig. 7(b); hereafter, we shall denote the irreducible interaction of Fig. 7(a) by the symbol $\mathcal{I}$.[12] Similarly, $\delta\Sigma/\delta G_n$ excludes the reducible graph of Fig. 4(b) which was retained in the definition of R.

The essential point is now the following: If our approximations are to be consistent, we must consider only those terms of $\partial\Sigma/\partial\epsilon$ which correspond to the graphs of γ and $\mathcal{I}$ retained in our weak coupling theory. These dominant graphs are

(i) for $\delta\Sigma/\delta G_n$, those which are reducible in channels 1 and 2, contributing to γ_1 and γ_2 [the only other graph included in γ is that of Fig. 4(b), which does not enter, since it is reducible in the third channel],

(ii) for $\delta\Sigma/\delta\mathcal{G}_m$, those of Fig. 7(c) [which, when iterated, generate the leading term of R shown on Fig. 4(b)].

In both cases, these graphs are obtained by opening a full or dashed line *belonging to an intermediate triplet* in the self-energy diagram [Fig. 8(a)]. We thus conclude that only energy derivation of the *triplet* lines will give a sizable contribution to $\partial\Sigma/\partial\epsilon$.[13] In Fig. 8(c), for instance, lines 1 and 2 belong to an intermediate triplet: When open, they give a contribution $\sim g^4L^3$ to $\partial\Sigma/\partial\epsilon$; in contrast, opening the "nontriplet" line 3 would only yield a negligible term $\sim g^4L$. We note that a given graph of Σ may contain many intermediate triplets, separated by irreducible "three-body" interaction kernels X [Fig. 8(b)]; when calculating $\partial\Sigma/\partial\epsilon$, we must open lines in each triplet: If we select one of them, we must allow for a complete γ on *both* sides [Fig. 8(a)].

The above analysis of "three-body" multiple scattering casts an interesting light on the nature of parquet graphs. A graph of γ may always be decomposed in the way of Fig. 9: An entrance vertex is followed by any number of irreducible three body kernels X. It is easily verified that the elementary parquet theory developed in I amounts to choosing for X the two graphs of Figs. 10(a) and 10(b) (I_1 and I_2 being the irreducible interactions in channels 1 and 2, calculated in the same approximation as γ). Thus, in the usual parquet approximation, the two full lines interact any number of times with the deep hole, in any order, but *always independently of each other*. There is no real "three-body process," as shown on Fig. 10(d), which would involve the three lines simultaneously. It is easily verified that the improved calculations of the present paper amounts to adding to X the graphs of Fig. 10(c).

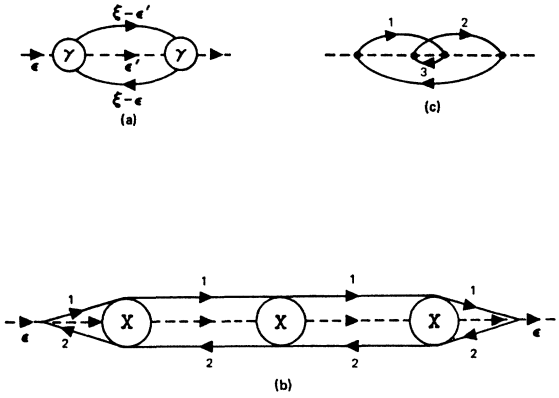

FIG. 8. (a) An intermediate triplet inside a self-energy graph. (b) A graph Σ may contain many intermediate triplets separated by "three-body" irreducible interactions X. (c) A specific example which shows both "triplet" electron lines 1 and 2, and a "nontriplet" line 3 (intermediate states are marked by dashed vertical lines); opening line 3 yields a negligible contribution to $\partial\Sigma/\partial\epsilon$.

[12] $\mathcal{I}$ enters the definition of γ only through those graphs which are reducible in the third channel (defined by the two dashed lines). One verifies easily that a graph reducible in channel 3 is necessarily irreducible in channels 1 and 2. A glance at Fig. 4(b) then shows that the only graph of $\mathcal{I}$ retained in our weak coupling approximation is that of Fig. 7(c). A higher-order graph like that of Fig. 7(d) is not included in building R and should be neglected.

[13] Intermediate triplets are known to control the spectral density $\mathrm{Im}\Sigma$ in the vicinity of the branch point (excitation of a single conduction electron by the deep hole is the process which is least affected by the phase-space restrictions due to energy conservation). $\partial\Sigma/\partial\epsilon$ may then be obtained from $\mathrm{Im}\Sigma$ using the appropriate Kramers-Kronig relation. It is tempting to claim that the leading role of intermediate triplets in $\partial\Sigma/\partial\epsilon$ arises from the same phase-space arguments that are involved for $\mathrm{Im}\Sigma$. Unfortunately, such a relationship does not exist, as shown by the counterexample of Fig. 8(c). Here, the importance of triplets arises from our *weak coupling* approximation, and not from phase-space restrictions.

We now return to the calculation of $\partial\Sigma/\partial\epsilon$: We must draw a continuous path from entrance to exit of the self-energy graph, and open only triplet lines along that path. We see on Fig. 8(b) that there are three obvious choices:

(1) Open the full lines marked "1" which run parallel to the deep propagator ($\eta_n=+1$).
(2) Open the full lines marked "2" running in the opposite direction ($\eta_n=-1$).
(3) Open the dotted line ($\eta_m=+1$).

Let us, for instance, take choice 1. It is clear that cutting any line "1" in Fig. 8(b) gives rise to a graph of γ_2—in fact, to all of them, once each. According to (38), we may, therefore, write

$$\frac{\partial\Sigma}{\partial\epsilon}=\frac{-i}{2\pi}\int d\epsilon_1\bar{\gamma}_2(\epsilon,\epsilon_1,\epsilon-\epsilon_1)\frac{\partial G(\epsilon_1)}{\partial\epsilon_1}, \tag{39}$$

where ϵ_1 is the energy of the open full line.[14] From (10), it follows that

$$\partial G/\partial\epsilon_1=2i\pi\nu_0\delta(\epsilon_1)$$

(deriving a full line amounts to setting its energy equal to zero). Hence, we find

$$\partial\Sigma/\partial\epsilon=\nu_0\bar{\gamma}_2(\epsilon). \tag{40a}$$

A similar calculation based on choice 2 would have yielded

$$\partial\Sigma/\partial\epsilon=-\nu_0\bar{\gamma}_1(\epsilon). \tag{40b}$$

In view of (23), the results (40a) and (40b) do indeed agree, and lead to the more explicit relation

$$\frac{\partial\Sigma}{\partial\epsilon}=\nu_0^2\int_0^t R^2(t')dt', \tag{41}$$

where $t(\epsilon)$ is the still unknown divergent parameter of our expansion.

We can also use choice 3, and open the intermediate dashed line in Fig. 8(a). We thus obtain

$$\frac{\partial\Sigma}{\partial\epsilon}=-\left(\frac{i}{2\pi}\right)^2\int d\epsilon'd\xi G(\xi-\epsilon)G(\xi-\epsilon')\frac{\partial\mathcal{G}}{\partial\epsilon'}[\gamma(\epsilon,\epsilon',\xi)]^2 \tag{42}$$

[in contrast to (27), (42) involves *two* factors γ, arising because we must open *any* intermediate triplet line]. If we note that

$$\partial\mathcal{G}/\partial\epsilon=\mathcal{G}(\epsilon)^2(1+\partial\Sigma/\partial\epsilon), \tag{43}$$

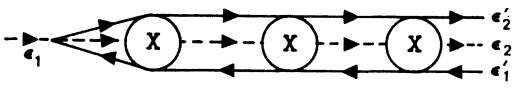

FIG. 9. General expansion of γ in terms of the irreducible three-body interaction X.

[14] The minus sign in (39) accounts for the breaking of a closed loop.

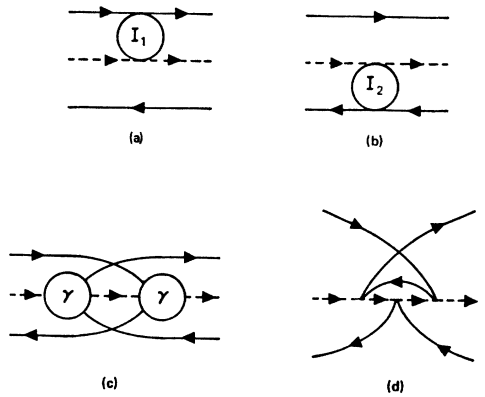

FIG. 10. Graphs contributing to the irreducible three body interaction X. (a) and (b) Contributions retained in the elementary parquet theory of I. (c) Additional graph involved in the present self-consistent formulation. (d) A negligible graph of X (the two full lines interact *together* with the dashed line).

we see that (42) is nothing but the usual Ward identity obeyed by $\partial\Sigma/\partial\epsilon$, written with our particular approximation to the irreducible interaction $\mathcal{I}$. It is difficult to evaluate (42) explicitly within our logarithmic accuracy, as it involves two factors $\mathcal{G}$ (it is not obvious how one can write the integral in terms of the divergent parameter t). On the other hand, (42) is useful in calculating the irreducible interaction R.

Besides the first-order vertex, R contains all the graphs of Fig. 4(b). Since the latter depend only on $\max(\epsilon_1,\epsilon_2)$, we may as well set $\epsilon_1=\epsilon_2=\epsilon$ in order to calculate their contribution; the corresponding assignment of energies is shown on Fig. 11. We also note that the right-hand-side bubble in Fig. 11 has comparable energies in its two singular channels: The corresponding factor γ reduces to its irreducible part $R(\epsilon')$. Figure 11 may then be transcribed into the following equation:

$$R(\epsilon)=V-\left(\frac{i}{2\pi}\right)^2\int d\epsilon'd\xi G(\xi-\epsilon)G(\xi-\epsilon')\times[\gamma(\epsilon,\epsilon',\xi)]^2R(\epsilon'). \tag{44}$$

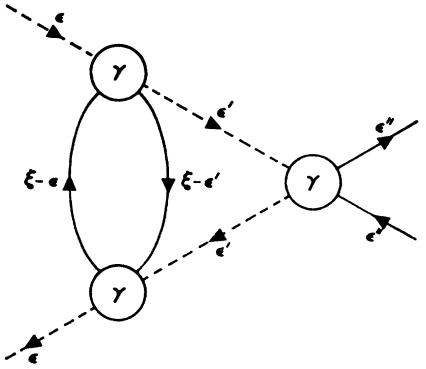

FIG. 11. The leading graph contributing to the totally irreducible interaction $R(\epsilon,\epsilon)$.

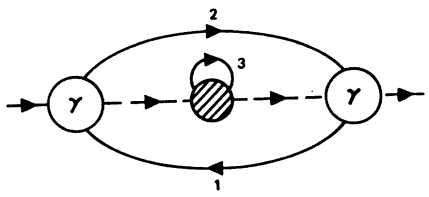

FIG. 12. A graph of γ is obtained by opening any G line in any graph of Σ. In our approximation, we only open lines belonging to an intermediate triplet. If we open lines 1 or 2, we obtain reducible graphs of, respectively, γ_1 and γ_2; the diagrams of R are obtained by opening line 3.

Comparing (44) with (42) and (43), we see at once that

$$R(\epsilon)=V[1+\partial\Sigma/\partial\epsilon]. \tag{45}$$

(45) is a simple form of the well-known Ward identity relating vertex and self-energy corrections. It shows that to a large extent the singularities in R and $\mathcal{G}$ will cancel each other.[15] Such a cancellation is, in fact, essential in our discussion of the higher-order graphs of R (see Appendix A).

Let us emphasize the absolute necessity for *consistent approximations* to the self-energy Σ and irreducible interaction R (such as to preserve the Ward identities). Because of the large amount of cancellation, one may get wild results if one normalizes Σ and not R. The general interaction operator γ is obtained by opening one full line in any graph of Σ; this line may belong to the skeleton graph itself, or to a self-energy insertion on some internal $\mathcal{G}$ (Fig. 12). We may thus write formally

$$\gamma=\left(\frac{\delta\Sigma}{\delta G}\right)_{\text{tot}}=\frac{\delta\Sigma}{\delta G}+\frac{\delta\Sigma}{\delta\mathcal{G}}\frac{\delta\mathcal{G}}{\delta G}. \tag{46}$$

As soon as we renormalize $\mathcal{G}$, it is essential to retain the last term of (46). If we assume from the outset that only triplet lines are important, we are led at once to the graphs of Fig. 4(b). If we were to improve on the calculation of $\partial\Sigma/\partial\epsilon$, we should automatically refine R in order to satisfy the general relation (46).

V. SOLUTION OF SELF-CONSISTENT EQUATIONS

We are now set up to calculate explicitly the unknown quantities R and t as a function of ϵ. We begin with R, which in view of (41) and (45) obeys the equation

$$R(t)=V\left[1+\nu_0{}^2\int_0^t R^2(t')dt'\right]. \tag{47}$$

The solution of (47) is straightforward [we derive (47) with respect to t and integrate the resulting differential equation]. We find

$$R(t)=V/(1-g^2t). \tag{48}$$

[15] Such a cancellation is obvious in the one-body approach of Ref. 6, where vertex and self-energy corrections are lumped into a single multiplicative factor.

We then proceed to calculate t. From (45) and (48), it follows that

$$1+\partial\Sigma/\partial\epsilon=1/(1-g^2t). \tag{49}$$

On the other hand, we know from (14) that

$$dt/d\epsilon=-\mathcal{G}(\epsilon)=1/(\epsilon+\tilde{\Sigma}). \tag{50}$$

By deriving (50) with respect to ϵ, and using (49), we obtain the following differential equation for the function $t(\epsilon)$:

$$t''/t'=t'/(1-g^2t). \tag{51}$$

The solution of (51) is elementary; we choose the constants of integration in such a way that

(i) $(1-g^2t)$ vanishes for $\epsilon=0$ (the singularity of $\partial\Sigma/\partial\epsilon$ must be at the branch point itself);

(ii) t vanishes for an energy $\epsilon\sim\xi_0$, where ξ_0 is the interaction cutoff. We thus find

$$\frac{\epsilon}{\xi_0}=\frac{[1-g^2t]^{(1+g^2)/g^2}}{1+g^2}. \tag{52}$$

Within our weak coupling approximation, we must neglect g^2 as compared to 1: (52) reduces to

$$1-g^2t=(\epsilon/\xi_0)^{g^2}. \tag{53}$$

Using (48) and (49), we then obtain the final explicit result:

$$1+\partial\Sigma/\partial\epsilon=R/V=(\xi_0/\epsilon)^{g^2}. \tag{54}$$

We note that t never diverges (it goes to $1/g^2$ when $\epsilon\to 0$): Nevertheless, the expansion remains singular, the actual expansion parameter being $1/(1-g^2t)$ rather than t. For moderately small energies, we may write (53) in the form

$$1-g^2t=\exp[g^2\ln(\epsilon/\xi_0)]=1-g^2\ln(\xi_0/\epsilon)+\cdots.$$

When $g^2L\ll 1$, we recover the usual logarithmic divergences of the elementary parquet theory.

The deep-level Green's function is obtained by integrating (54); neglecting corrections of order g^2, we find

$$\mathcal{G}(\epsilon)=-(\epsilon+\tilde{\Sigma})^{-1}=-(\epsilon^{-1})(\epsilon/\xi_0)^{g^2}. \tag{55}$$

The singularity at $\epsilon=0$ is *weakened* by renormalization. Similarly, we may calculate the x-ray response function $\chi(\omega)$, given by (36). The function $Q(t)$ is defined in (29), and is obtained by integrating (68):

$$Q(t)=-(1/g)\ln[1-g^2t]. \tag{56}$$

The integral (36) is then straightforward and yields

$$\chi(\omega)=[\nu_0/(2g-g^2)]\{(\xi_0/\omega)^{2g-g^2}-1\}. \tag{57}$$

Within our approximations, we must neglect g^2 as compared to g, so that

$$\chi(\omega)=\frac{\nu_0}{2g}\left\{\left(\frac{\xi_0}{\omega}\right)^{2g}-1\right\}. \tag{58}$$

The x-ray transition rate is thus unaffected by a self-consistent vertex and self-energy renormalization—at least in the weak coupling limit. Actually, the "one-body" approach of Ref. 4 shows that the term g^2 in the exponent of (57) is meaningful: Renormalization thus reduces the Mahan singularity near $\omega=0$. Physically, a renormalization of $\mathcal{G}$ broadens the deep level, so that the resonance in χ is quenched.

The spectral densities $\mathrm{Im}\mathcal{G}$ and $\mathrm{Im}\chi$ may be calculated by the same method as in I. We know that the branch cuts of $\mathcal{G}$ and χ extend on one side only of their respective branch points (E for $\mathcal{G}$, ω_0 for χ). Thus, $\mathrm{Im}\mathcal{G}$ and $\mathrm{Im}\chi$ are *step functions* of the energy: The determination of the factors ϵ^α in (55) and (58) is then completely determined; on the branch cut side they involve a factor

$$(-1)^\alpha=\cos\pi\alpha+i\sin\pi\alpha\approx 1+i\pi\alpha$$

(assuming $\alpha\ll 1$). In the weak coupling limit, we thus find[16]

$$\begin{aligned}\mathrm{Im}\mathcal{G}&=(\pi g^2/\epsilon)(\epsilon/\xi_0)^{g^2}\eta(\pm\epsilon)\,,\\ \mathrm{Im}\chi&=\pi\nu_0(\xi_0/\omega)^{2g}\eta(\pm\omega)\,.\end{aligned}\tag{59}$$

$\eta(x)$ is the step function; ϵ and ω are measured from the appropriate branch points.

All the above analysis was carried out for spinless electrons. The inclusion of spin is straightforward if we assume that the basic interaction in (1) conserves the spin of conduction electrons. Put another way, we consider only *direct scattering* on the deep hole, and ignore any exchange process in which both the conduction and the deep electrons would flip their spin. (Such a restriction is essential if we wish to consider only a *single* deep level.) The interaction operator is then diagonal in the spin variables; the conduction-electron spin is conserved along any sequence of *full lines*, whether open or constituting a closed loop. For an open line, the spin is fixed by the component of γ which we consider, and thus our previous calculation remains valid [for instance, the general equations (33) and (34) are unaffected]. On the other hand, the spin of a closed loop is arbitrary: The corresponding contribution must be doubled. Such closed loops enter only in the self-energy graphs of Fig. 8(a), and in the vertex correction of Fig. 4(b). The only effect of spin is thus to add a factor 2 on the right-hand side of (41) [the relation (65) between R and Σ is unaffected]. From there on, the solution proceeds as before; the only difference is that all factors g^2 are replaced by $2g^2$ (the exponent $2g$ appearing in χ is unaffected, since it arises from a summation of *open* line contributions). For instance, (59) is replaced by

$$\begin{aligned}\mathrm{Im}\mathcal{G}&=(2\pi g^2/\epsilon)(\epsilon/\xi_0)^{2g^2},\\ \mathrm{Im}\chi&=\pi\nu_0(\xi_0/\omega)^{2g}.\end{aligned}\qquad\text{(spin included)}\tag{60}$$

[16] For a more detailed discussion, see (I.43)–(I.45).

The transposition of our algebra is trivial, and is not worth a detailed discussion.

VI. CONCLUSION

The self-consistent approach of this paper provides an explicit expression for the deep-level Green's function $\mathcal{G}(\epsilon)$, which agrees with the conjectures of Anderson and Hopfield.[17] As could be expected, the spectral density of $\mathcal{G}$ is broadened asymmetrically, the continuum corresponding to virtual excitation of conduction electrons by the deep hole. We note that the spectral density $\mathrm{Im}\mathcal{G}$ remains infinite at $\epsilon=0$: As a consequence, the Fourier transform $\mathcal{G}(t)$ decays very slowly. From (60), we verify that

$$\mathcal{G}(t)\sim(\xi_0 t)^{-2g^2}.$$

Such a slow decay arises from the long time required by electrons near the Fermi surface to adjust to their new environment.

The only quantity measured experimentally is the x-ray response function $\chi(\omega)$. We have shown that in the weak coupling limit, χ is unaffected by renormalization: We thus substantiate the predictions of Mahan[2] concerning the singularity of the x-ray emission and absorption spectra near threshold.[18] Our result (57) suggests that, in a more accurate calculation, the broadening of $\mathcal{G}$ should act to decrease the Mahan singularity in χ. Such a contention is, in fact, borne out by the exact "one-body" treatment of Ref. 4. For large coupling strength, the broadening of $\mathcal{G}$ may even overcome the Mahan singularity, leading to zero amplitude at threshold instead of a divergence. Unfortunately, the latter result lies outside the scope of the present many-body approach, which can be pursued only in the weak coupling limit ($g\ll 1$).

The major interest of the paper lies in the method more than in the results. On a simple example, we have shown how to treat divergent fluctuations in *self-consistent fashion*. The fluctuations modify the deep-level propagator, which in turn reacts on the fluctuation amplitude. We have set a pattern to treat the divergences self-consistently and shown how important it is to maintain coherent approximations in evaluating self-energy and vertex corrections. Such an approach generalizes the well-known parquet theory and should prove useful in any one-dimensional problem involving divergent fluctuations: one-dimensional superconductivity,[8] Kondo effect[7] (where the relevant dimension is the time, as in the present problem). Of course, the cancellations noticed in this paper may not occur in more complicated problems; yet the same general approach is applicable.

[17] P. W. Anderson, Phys. Rev. Letters **18**, 1069 (1967); J. J. Hopfield (private communication).

[18] We note that $\mathcal{G}$ and χ involve different exponents, respectively, $2g^2$ and $2g$: There is no contradiction between the results of Mahan (for χ) and of Anderson (for $\mathcal{G}$).

ACKNOWLEDGMENTS

The authors express their gratitude to Professor A. A. Abrikosov and I. E. Dzyaloshinski for an enlightening discussion and correspondence and especially for pointing out the need for a systematic approximation scheme throughout the theory. One of us (P. N.) wishes to thank his colleagues of the Department of Physics in La Jolla for their hospitality during the Spring of 1968.

APPENDIX A: HIGHER-ORDER GRAPHS OF R

It is customary to define *skeleton* graphs of γ, which contain no self-energy insertion on any of the internal lines. The complete γ is obtained by assigning to each line a renormalized propagator $\mathcal{G}$, instead of the unperturbed $\mathcal{G}$. In the same spirit, let us define a still smaller set of *fundamental interaction graphs* (of order ≥ 2), such that by replacing each line by a factor $\mathcal{G}$ and *each vertex by a full factor* γ, one obtains the complete interaction operator (except, of course, its first-order term). Topologically, these graphs are such that they cannot be split in two independent parts (of order >1) by cutting at most two full lines and two dotted lines[19] (otherwise, the graph would already appear in the vertex renormalization of some lower-order term). The only fundamental graphs of order 2, 3, 4 are those of Fig. 13 (in fifth order their number is much larger[20]).

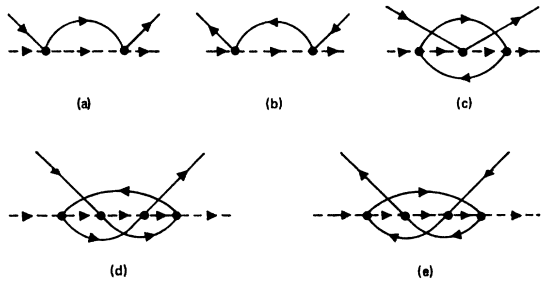

FIG. 13. The fundamental interaction graphs through fourth order.

We shall first discuss the contribution of fundamental graphs to R, and then examine what happens when the propagators *and vertices* are renormalized.

We consider a fundamental graph of order n, containing $n-1$ internal full lines. The dotted line runs in a given time direction—say forward; each full line, with momentum k_i, is either parallel to the dotted line ($\epsilon_{k_i}>0$) or antiparallel ($\epsilon_{k_i}<0$). We shall set

$$E_i=+\epsilon_{k_i} \quad \text{(parallel lines)}$$
$$=-\epsilon_{k_i} \quad \text{(antiparallel lines)}.$$

The momentum summation involves an integration over all E_i from 0 to the cutoff ξ_0. We note that the graph contains $n-1$ *intermediate states* (involving a number of electrons and holes) whose energy ϵ_α is a sum of the relevant E_i. Let us assume that the four external energies of the operator γ are zero (which is enough to find the *number* of divergent logarithms). We may perform the energy integrations inside the diagram, and express its contribution in the form

$$\int_0^{\xi_0} \frac{dE_1\cdots dE_{n-1}}{\alpha_1\cdots\alpha_{n-1}}. \tag{A1}$$

The expression (A1) is familiar in the time-independent formalism of Hugenholtz and Van Hove.[21]

If one denominator α contains a single term E_i, the integral over dE_i diverges near the origin and leads to a logarithmic factor. More generally, let us consider a *set* S_p of p intermediate states whose energies α involve various combinations of *the same* p energies $E_1\cdots E_p$; we assume that no smaller subset $S_{p'}$ can be picked out of S_p; a typical set S_3 might involve, for instance, energy denominators of the form

$$\frac{1}{(E_1+E_2)(E_1+E_2+E_3)(E_1+E_3)}.$$

It is clear that the integration over $dE_1\cdots dE_p$ diverges near the origin $E_1=\cdots=E_p=0$, and thereby leads to *one* logarithmic factor. The number of logs present in an arbitrary graph of γ may then be obtained in the following way:

(i) Find all sets S_1, x_1 in number; set the energies E_i of their lines equal to zero.

(ii) Among the remaining intermediate states, find all x_2 sets S_2; set the energies of their lines equal to zero.

etc.

The net number of logarithms is $x_1+x_2+\cdots+x_{n-1}$. We note that any graph of order n will contain at least one singular set S_{n-1} (if it has none smaller): All terms of γ thus have *at least one* logarithmic factor.

We now prove that a *fundamental* graph containing a set S_p is necessarily of order $(p+1)$. The p lines of S_p touch the dashed line on simple vertices (because the graph is fundamental). $(p-1)$ of these vertices are required to separate the p intermediate states from each other: They will require $(2p-2)$ line extremities. The latter are to be found among

(i) the $2p$ ends of the lines of S_p,
(ii) possibly, one or two of the external lines.

Let us, for instance, assume that the two external lines are attached to the $(p-1)$ internal vertices. Then the set S_p is connected to the rest of the diagram by *four* lines only, two of which must be on the right and two

[19] See, for instance, C. T. de Dominicis and P. C. Martin, J. Math. Phys. **5**, 131 (1964).

[20] The second-order graphs of Fig. 13 must be treated separately, as replacement of the *two* vertices by *full* operators γ would lead to diagram duplication. This duplication is avoided by writing the appropriate Bethe-Salpeter equations. Such a difficulty does not occur for higher fundamental graphs.

[21] N. M. Hugenholtz and L. Van Hove, Physica **24**, 363 (1958).

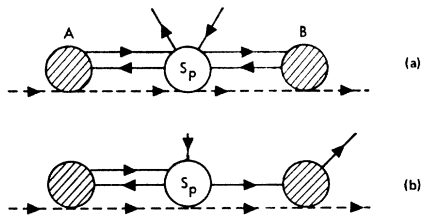

FIG. 14. (a) A set S_p (coupled to the two external lines) is connected to the rest of the diagram by only *four* lines, two on the right and two on the left. If the whole graph is fundamental the kernels A and B must reduce to single vertices. The external lines cannot be attached to some other part of the graph, as shown on Fig. 14(b).

on the left [Fig. 14(a)]. If the whole graph is to be fundamental, the kernels A and B on Fig. 14(a) must reduce to single vertices: The total graph is of order $(p+1)$. In the same way, one shows that the external lines could not be attached to some other part of the diagram [Fig. 14(b)]. Our theorem is thus proved, and leads to the conclusion that fundamental diagrams involve only *one* divergent logarithm. In the weak coupling limit, we may retain the lowest-order graph of Fig. 13(c) [since the diagrams of Figs. 13(a) and (b) cancel each other].

Let us consider an arbitrary fundamental graph of order $(p+1)$: The total interaction operator is obtained by affixing

(i) a factor $\mathcal{G}$ to each of the p dashed lines,
(ii) a factor γ to each of the $(p+1)$ vertices.

Since we integrate over all internal energies, the factors γ will involve comparable energies in the two channels: They may be replaced by the irreducible interaction R. We then use (45) and remark that the singularities in R and $\mathcal{G}$ will cancel each other; the net contribution of the fundamental graph will be of order

$$g^p R.$$

Again, we need only retain the lowest-order nonzero contribution, i.e., the term $p=2$. We have thus justified our approximation to the irreducible interaction R, involving only the graph of Fig. 11.

APPENDIX B: LOGARITHMIC APPROXIMATIONS

Equations (8) may be written formally as

$$\begin{aligned}\gamma_1&=I_1X_1I_1+I_1X_1I_1X_1I_1+\cdots=I_1X_1\gamma,\\ \bar\gamma_2&=\bar I_2X_2\bar I_2+\bar I_2X_2\bar I_2X_2\bar I_2+\cdots=\bar I_2X_2\bar\gamma,\end{aligned}\tag{B1}$$

where the kernels X_i stand for the product $\mathcal{G}G$. Our logarithmic approximation involved an error δX_i on X_i, as well as an error on the *functional dependence* of I_i on γ_i. The actual I_i is given by

$$I_i=f(\gamma_i)+\delta f(\gamma_i).\tag{B2}$$

To lowest order, the corresponding error on I_i is

$$\delta I_i=(\partial f/\partial\gamma_i)\delta\gamma_i+\delta f_i.\tag{B3}$$

The *first-order* correction to γ_1 is obtained by modifying any factor X_1 or I_1 in (B1); we verify easily that

$$\delta\gamma_1=\gamma\delta X_1\gamma+\delta I_1X_1\gamma+\gamma X_1\delta I_1+\gamma X_1\delta I_1X_1\gamma.\tag{B4}$$

(A similar equation holds for $\delta\bar\gamma_2$.) If we replace δI_1 by its expression (B3), we obtain two coupled integral equations for $\delta\gamma_1$ and $\delta\bar\gamma_2$, which are "driven" by the inhomogeneous terms

$$\phi_i=\gamma\delta X_i\gamma+\delta f_iX_i\gamma+\gamma X_i\delta f_i+\gamma X_i\delta f_iX_i\gamma.\tag{B5}$$

To be more specific, let us consider the simple case $t_1=t_2=\alpha=\beta$ (all energies are comparable). The various factors γ in (B4) are then given by (32). On expliciting the integrals, we obtain the following equations for the corrections $\delta\gamma_1(\alpha)$ and $\delta\bar\gamma_2(\alpha)$:

$$\begin{aligned}\delta\gamma_1(\alpha)&=\phi_1(\alpha)-2\nu_0\int_0^\alpha dt\,R(t)\exp[Q(t)-Q(\alpha)]\delta\bar\gamma_2(t)\\ &\quad+\nu_0^2\int_0^\alpha dt\,dt'R(t)R(t')\delta\bar\gamma_2(\min(t,t'))\\ &\qquad\times\exp[Q(t)+Q(t')-2Q(\alpha)],\\ \delta\bar\gamma_2(\alpha)&=\phi_2(\alpha)+2\nu_0\int_0^\alpha dt\,R(t)\exp[Q(\alpha)-Q(t)]\delta\gamma_1(t)\\ &\quad+\nu_0^2\int_0^\alpha dt\,dt'R(t)R(t')\delta\gamma_1(\min(t,t'))\\ &\qquad\times\exp[2Q(\alpha)-Q(t)-Q(t')].\end{aligned}\tag{B6}$$

In the last terms of (B6), we make the replacement

$$\int_0^\alpha dt\,dt'=2\int_0^\alpha dt\int_0^t dt'$$

and integrate by parts with respect to t. On making use of (29), we find

$$\begin{aligned}\delta\gamma_1(\alpha)&=\phi_1(\alpha)-2\nu_0\int_0^\alpha R(t)\delta\bar\gamma_2(t)\\ &\qquad\times\exp[2Q(t)-2Q(\alpha)]dt,\\ \delta\bar\gamma_2(\alpha)&=\phi_2(\alpha)+2\nu_0\int_0^\alpha R(t)\delta\gamma_1(t)\\ &\qquad\times\exp[2Q(\alpha)-2Q(t)]dt.\end{aligned}\tag{B7}$$

In order to solve (B7), we multiply the two equations by $e^{\pm2Q(\alpha)}$, and derive, with respect to α, which yields

$$\begin{aligned}\delta\gamma_1'+2\nu_0R[\delta\gamma_1+\delta\bar\gamma_2]&=\phi_1'+2\nu_0R\phi_1,\\ \delta\bar\gamma_2'-2\nu_0R[\delta\gamma_1+\delta\bar\gamma_2]&=\phi_2'-2\nu_0R\phi_2.\end{aligned}\tag{B8}$$

From (B8), it follows that

$$\delta\gamma_1+\delta\bar{\gamma}_2=\int_0^\alpha 2\nu_0 R(t)dt[\phi_1(t)-\phi_2(t)] +\phi_1(\alpha)+\phi_2(\alpha). \quad \text{(B9)}$$

Our logarithmic approximations are correct if the error (B9) is negligible as compared to the main term $\gamma(\alpha)=R(\alpha)$.

In evaluating ϕ_1 and ϕ_2, we consider first the errors δX_i. Part of the error arises from our approximation (12) to the exact conduction propagator (10); we may write it as

$$\delta X_i(\epsilon)\sim u_i(\epsilon)X_i(\epsilon), \quad \text{(B10)}$$

where u_i contains terms of order g^2, and also a "regular" term of order

$$\ln\left|\frac{\xi_0-\epsilon}{\xi_0+\epsilon}\right| \operatorname{sgn}\epsilon$$

(only the even part of $u_i(\epsilon)$ contributes to the integral). The remaining error lies in our neglect of $\mathrm{Im}\mathcal{G}$. If $\mathcal{G}$ is not renormalized, the corresponding contribution is localized at $\epsilon_i=0$, and gives a correction to γ of order g^2, thus negligible. If we introduce self-energy and vertex renormalization, $\mathrm{Im}\mathcal{G}$ is given by (59), and is of order

$$\mathrm{Im}\mathcal{G}\sim g^2\mathcal{G}\eta(\epsilon)$$

(where η is a step function). The corresponding correction has again the form (B10).

The other terms of ϕ_1 and ϕ_2 involve the errors δf_i on the interaction kernels. The latter exist only when the energies on both sides of δf_i are comparable (otherwise, the logarithmic approximation is excellent). In the last term of (B5), for instance, we may write

$$X_i(\epsilon)\delta f_i(\epsilon,\epsilon')X_i(\epsilon')\sim g^2X_i(\epsilon)\delta(\epsilon-\epsilon'). \quad \text{(B11)}$$

(The error in δf is necessarily of second order, and, moreover, the self-energy and vertex corrections cancel each other.) The correction (B11) may thus be expressed in the general form (B10).

If we carry (B10) into (B5), we find

$$\phi_1=\nu_0\int_0^\alpha R^2(t)e^{2[Q(t)-Q(\alpha)]}u_1(\epsilon)dt,$$
$$\phi_2=\nu_0\int_0^\alpha R^2(t)e^{2[Q(\alpha)-Q(t)]}u_2(\epsilon)dt. \quad \text{(B12)}$$

From (B12), it follows at once that

$$\phi_1'+2\nu_0R\phi_1=\nu_0R(\alpha)^2u_1(\xi),$$
$$\phi_2'-2\nu_0R\phi_2=\nu_0R(\alpha)^2u_2(\xi), \quad \text{(B13)}$$

which, together with (B8), leads to

$$\delta\gamma_1+\delta\bar{\gamma}_2\sim\int_0^\alpha \nu_0R(t)^2[u_1(\epsilon)+u_2(\epsilon)]dt. \quad \text{(B14)}$$

The terms of u of order g^2 contribute to (B14) a correction $\lesssim gR$, which is negligible as compared to R. [Actually, the correction is of order g^2R, because of the symmetry condition (I.22) established in the preceding paper.] The other terms of u, arising from the *real* part of G, are not singular at $\epsilon=0$: In the integral (B14), they contribute only when $t\approx 0$, giving a negligible correction $\lesssim g^2$. Similar arguments may be used to discard the contribution of the second and third terms of (B5).

A rigorous appraisal of all these approximations is extremely fastidious: Here we have only sketched the main line of the argument. Our only purpose was to convey two important points:

(i) The logarithmic errors in $\gamma(\xi)$ are always smaller than the main term $R(\xi)$ which we have retained, by a factor $\lesssim g$ (in fact, g^2 because of the symmetry requirement).

(ii) There is no accumulation of logarithms in the correction terms. The origin of the latter simplification lies in the feedback of $\delta\gamma_1$ and $\delta\bar{\gamma}_2$ on each other. The two terms are coupled through (B6), and this coupling provides a large stability against errors in X_i or I_i. This "built-in" stability may be traced to the cancellation of singularities between the two channels, and to the compensation of vertex and self-energy corrections.